

The Banki Water Turbine

By

C. A. MOCKMORE
Professor of Civil Engineering

and

FRED MERRYFIELD
Professor of Civil Engineering

Bulletin Series No. 25

February 1949

Engineering Experiment Station
Oregon State System of Higher Education
Oregon State College
Corvallis

The Banki Water Turbine

By

C. A. MOCKMORE

Professor of Civil Engineering

and

FRED MERRYFIELD

Professor of Civil Engineering

Bulletin Series No. 25

February 1949

Engineering Experiment Station
Oregon State System of Higher Education
Oregon State College
Corvallis

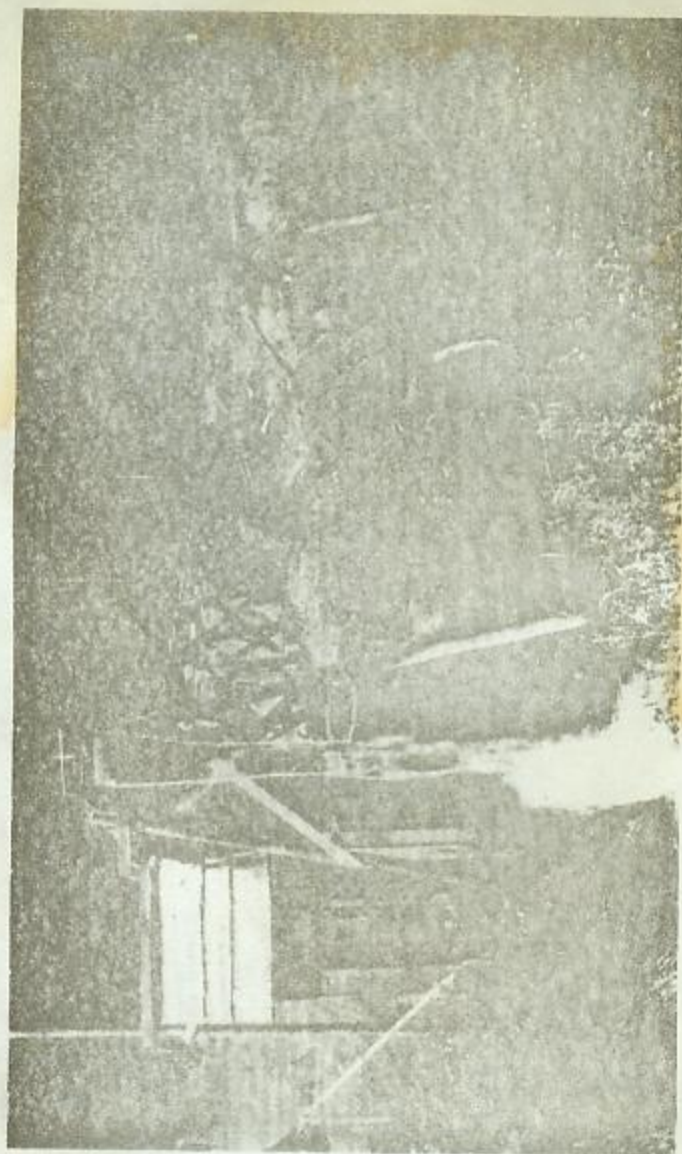


Figure 1. Typical small water turbine installation.

TABLE OF CONTENTS

	Page
I. Introduction	5
1. Introductory Statement	5
II. Theory of the Banki Turbine	5
1. Description of Turbine	5
2. Path of Jet through Turbine	6
3. Efficiency	7
4. Construction Proportions	10
(A) Blade Angle	10
(B) Radial Rim Width	10
(C) Wheel Diameter and Axial Wheel Breadth	14
(D) Curvature of the Blade	15
(E) Central Angle	15
III. Design of Laboratory Turbine	16
1. Assumed Design Data	16
2. Breadth and Diameter of Wheel	17
3. Speed of Wheel	17
4. Thickness of Jet	17
5. Spacing of Blades in Wheel	17
6. Radial Rim Width	18
7. Radius of Blade Curvatures	18
8. Distance of Jet from Center of Shaft	18
9. Distance of Jet from Inner Periphery of Wheel	18
10. Construction of the Wheel	18
11. Laboratory Tests	18
IV. Discussion	19
1. Limitations of Tests	19
2. Power	19
3. Quantity	19
4. Speed	19
5. Efficiency-Speed	19
6. Efficiency-Power	23
7. Specific Speed	23
V. The Turbine Nozzle	23
1. Test Nozzle	23
2. German Nozzles	23
VI. Installations	26
1. European Turbines	26
2. American Installations	26
VII. Conclusions	27

ILLUSTRATIONS

	Page
Figure 1. Typical Small Water Turbine Installation	6
Figure 2. Path of Water through Turbine	6
Figure 3. Interference of Filaments of Flow through Wheel	8
Figure 4. Velocity Diagram	8
Figure 5. Blade Spacing	9
Figure 6. Composite Velocity Diagram	11
Figure 7. Velocity Diagrams	11
Figure 8. Path of Jet inside Wheel	13
Figure 9. Curvature of Blades	16
Figure 10. Power Curves for Banki Turbine under 16-ft Head	20
Figure 11. Efficiency Curves for Banki Turbine under 16-ft Head	21
Figure 12. Characteristic Curves for Banki Turbine under 16-ft Head	22
Figure 13. Banki Water Turbine Built in Oregon State College Hydraulics Laboratory	23
Figure 14. German Design of Banki Turbine and Nozzle	24
Figure 15. Alternate German Design of Banki Turbine and Nozzle	25
Figure 16. Banki Turbine Runner and Nozzle	26
Figure 17. Inside of Powerhouse, Showing Jackshaft and Generator Driven by Banki Turbine	27

The Banki Water Turbine

By

C. A. MOCKMORE

Professor of Civil Engineering

and

FRED MERRYFIELD

Professor of Civil Engineering

I. INTRODUCTION

1. **Introductory statement.** The object of this Bulletin is to present a free translation of Donat Banki's paper "Neue Wasser-turbine," and to show the results of a series of tests on a laboratory turbine built according to the specifications of Banki.

The Banki turbine is an atmospheric radial flow wheel which derives its power from the kinetic energy of the water jet. The characteristic speed of the turbine places it between the so-called Pelton tangential water turbine and the Francis mixed-flow wheel. There are some unusual characteristics not found in most water wheels which are displayed by the Banki turbine and should be of interest to most engineers, especially those of the Mountain States.

Included in this bulletin are diagrams of two Banki turbine nozzles as patented and used in Europe.

II. THEORY OF THE BANKI TURBINE

1. **Description of turbine.** The Banki turbine consists of two parts, a nozzle and a turbine runner. The runner is built up of two parallel circular disks joined together at the rim with a series of curved blades. The nozzle, whose cross-sectional area is rectangular, discharges the jet the full width of the wheel and enters the wheel at an angle of 16 degrees to the tangent of the periphery of the wheel. The shape of the jet is rectangular, wide, and not very deep. The water strikes the blades on the rim of the wheel (Figure 2), flows over the blade, leaving it, passing through the empty space between the inner rims, enters a blade on the inner side of the rim, and discharges at the outer rim. The wheel is therefore an inward jet wheel and because the flow is essentially radial, the diameter of the wheel is practically independent of the amount of water impact, and the desired wheel breadth can be given independent of the quantity of water.

2. Path of jet through turbine. Assuming that the center of the jet enters the runner at point A (Figure 2) at an angle of with the tangent to the periphery, the velocity of the water before entering would be

$$V_1 = C(2gH)^{\frac{1}{2}} \quad (1)$$

V_1 = Absolute velocity of water

H = Head at the point

C = Coefficient dependent upon the nozzle

The relative velocity of the water at entrance, v_1 , can be found if u_1 , the peripheral velocity of the wheel at that point, is known. β_1 would be the angle between the forward directions of the two latter

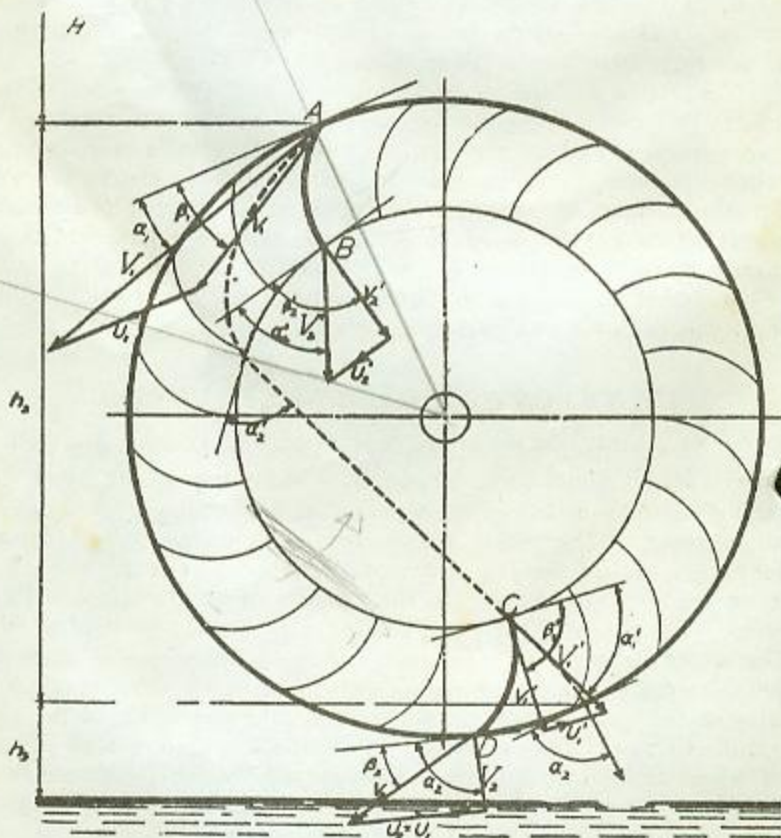


Figure 2. Path of water through turbine.

primes
refer to inside
of runner
① - inlet to
② - exit to
blade

velocities. For maximum efficiency, the angle of the blade should equal β_1 . If AB represents the blade, the relative velocity at exit, v_2' , forms β_2' with the peripheral velocity of the wheel at that point. The absolute velocity of the water at exit to the blade, V_2' , can be determined by means of v_2' , β_2' , and u_2 . The angle between this absolute velocity and the velocity of the wheel at this point is α_2' . The absolute path of the water while flowing over the blade AB can be determined as well as the actual point at which the water leaves the blade. Assuming no change in absolute velocity V_2' , the point C , where the water again enters the rim, can be found. V_2' at this point becomes V_1' , and the absolute path of the water over the blade CD from point C to point D at discharge can be ascertained.

Accordingly $\alpha_1' = \alpha_2'$

$$\beta_1' = \beta_2'$$

$$\beta_1 = \beta_2$$

$$\Sigma \bar{F} = \int_{CS} \rho \bar{V} (\bar{V} \cdot \bar{n}) dA$$

$$\dot{Q} - \dot{W}_S = \int_{CS} \left(\frac{V^2}{2} + \frac{p}{\rho} + gz + \bar{u} \right) \rho \bar{V} \cdot \bar{n} dA$$

since they are corresponding angles of the same blade.

It is apparent that the whole jet cannot follow these paths, since the paths of some particles of water tend to cross inside the wheel, as shown in Figure 3. The deflection angles θ and θ_1 will be a maximum at the outer edge of each jet. Figure 3 shows the approximate condition.

3. Efficiency. The following equation for brake horsepower is true:

$$HP = \left[\frac{\dot{W}}{g} (V_1 \cos \alpha_1 + V_2 \cos \alpha_2) u_1 \right] \frac{\text{Disc}}{\text{Time}} \quad (2)$$

Part of the formula (2) can be reduced by plotting all the velocity angles as shown in Figure 3.

$$V_2 \cos \alpha_2 = v_2 \cos \beta_2 - u_1 \quad (3)$$

Neglecting the increase in velocity of water due to the fall h_2 (Figure 2) which is small in most cases,

$$v_2 = \psi v_1 \quad (4)$$

where ψ is an empirical coefficient less than unity (about 0.98). From the velocity diagram Figure 4,

$$v_1 = (V_1 \cos \alpha_1 - u_1) / (\cos \beta_1) \quad (5)$$

Substituting equations (3), (4), and (5) in the horsepower equation (2)

$$HP \text{ output} = (WQ u_1 / g) (V_1 \cos \alpha_1 - u_1) \times (1 + \psi \cos \beta_2 / \cos \beta_1) \quad (6)$$

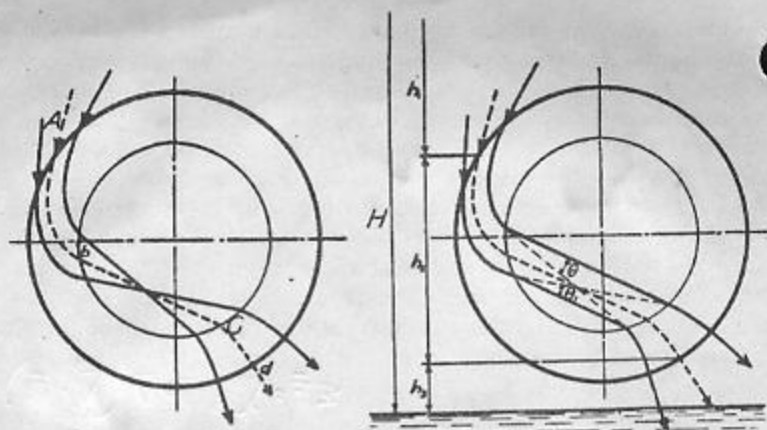


Figure 3. Interference of filaments of flow through wheel.

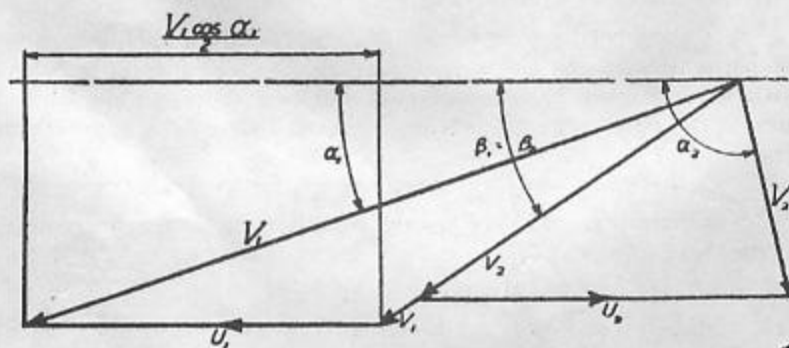


Figure 4. Velocity diagram

The theoretical horsepower input due to the head H_1

$$HP = wQH/g = wQV_1^2/C^2 2g \quad (7)$$

The efficiency, e , is equal to the ratio of the output and input horsepower,

$$e = (2C^2 u_1/V_1) (1 + \psi \cos \beta_2 / \cos \beta_1) \times (\cos \alpha_1 - u_1/V_1) \quad (8)$$

when

$$\beta_2 = \beta_1, \text{ then efficiency} \\ e = (2C^2 u_1/V_1) (1 + \psi) (\cos \alpha_1 - u_1/V_1) \quad (9)$$

Considering all variables as constant except efficiency and u_1/V_1 , and differentiating and equating to zero, then

$$u_1 V_1 = \cos \alpha_1 / 2 \quad (10)$$

and for maximum efficiency

$$e_{max} = \frac{1}{2} C^2 (1 + \psi) \cos^2 \alpha_1 \quad (11)$$

It is noticeable (see Figure 4) that the direction of V_2 when $u_1 = \frac{1}{2} V_1 \cos \alpha_1$, does not become radial. The outflow would be radial with

$$u_1 = [C/(1 + \psi)] (V_1 \cos \alpha_1) \quad (12)$$

only when ψ and C are unity, that is, assuming no loss of head due to friction in nozzle or on the blades. To obtain the highest mechanical efficiency, the entrance angle α_1 should be as small as possible, and an angle of 16° can be obtained for α_1 without difficulty. For this value $\cos \alpha_1 = 0.96$, $\cos^2 \alpha_1 = 0.92$.

Substituting in equation (11), $C = 0.98$ and $\psi = 0.98$, the maximum efficiency would be 87.8 per cent. Since the efficiency of the

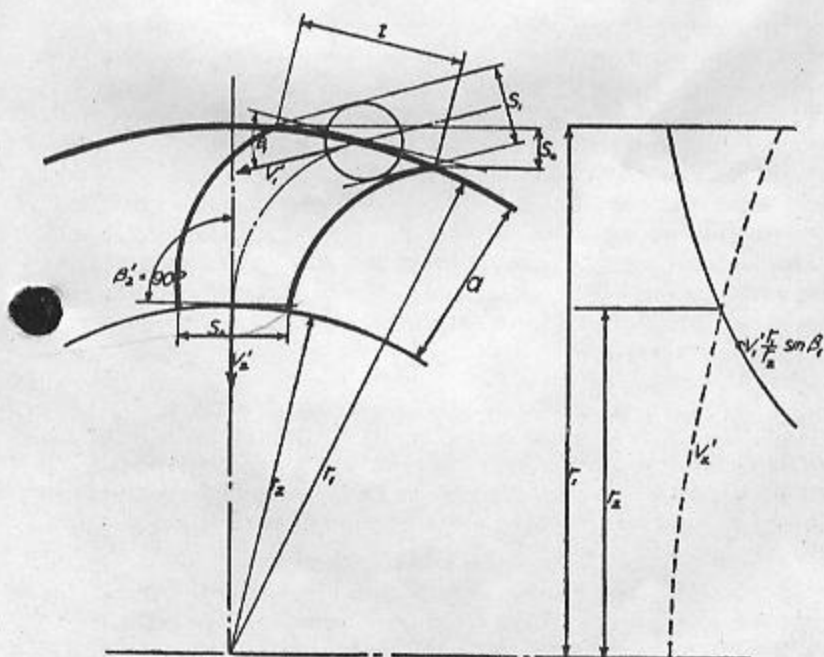


Figure 5. Blade spacing.

nozzle varies as the square of the coefficient, the greatest care should be taken to avoid loss here. There are hydraulic losses due to water striking the outer and inner periphery. The latter loss is small, for according to computations to be made later, the original thickness of the jet s_0 , Figure 5, increases to 1.90, which means that about 72 per cent of the whole energy was given up by the water striking the blade from the outside and 28 per cent was left in the water prior to striking the inside periphery. If the number of blades is correct and they are as thin and smooth as possible the coefficient ψ may be obtained as high as 0.98.

4. Construction proportions.

(A) Blade angle: The blade angle β_1 , can be determined from α_1 , V_1 , and u_1 in Figures 2 and 4.

$$\text{If } u_1 = \frac{1}{2}V_1 \cos \alpha_1 \quad (10)$$

$$\text{then } \tan \beta_1 = 2 \tan \alpha_1 \quad (13)$$

assuming $\alpha_1 = 16^\circ$

then $\beta_1 = 29^\circ 50'$ or 30° approx.

The angle between the blade on the inner periphery and the tangent to the inner periphery β_2 can be determined by means of the following as shown in Figure 6. Draw the two inner velocity triangles together by moving both blades together so that point C falls on point B and the tangents coincide. Assuming that the inner absolute exit and entrance velocities are equal and because $\alpha_2' = \alpha_1'$ the triangles are congruent and v_2' and v_1' fall in the same direction.

Assuming no shock loss at entrance at point C then $\beta_2' = 90^\circ$, that is, the inner tip of the blade must be radial. On account of the difference in elevation between points B and C (exit and entrance to the inner periphery) V_1' might differ from V_2' if there were losses between these points.

$$V_1' = [2gh_2 + (V_2')^2]^{\frac{1}{2}} \quad (14)$$

Assuming $\beta_2' = 90^\circ$ (Figure 7a) v_1' would not coincide with the blade angle and therefore a shock loss would be experienced. In order to avoid this β_2 must be greater than 90° . The difference in V_2' and V_1' however is usually small because h_2 is small, so β_2 might be 90° in all cases.

(B) Radial rim width: Neglecting the blade thickness, the thickness (s_1) Figure 5, of the jet entrance, measured at right angles to the relative velocity, is given by the blade spacing (t).

$$s_1 = t \sin \beta_1 \quad (15)$$

It is not advisable to increase the rim width (a) over this limit because the amount of water striking it could not flow through so small a cross-section and back pressure would result. Moreover, a rim width which would be under this limit would be inefficient since separated jets would flow out of the spacing between the blades at the inner periphery.

In order to determine the width (a) it is necessary to know the velocity v_2' , which is affected by the centrifugal force (see Figure 5).

$$(v_1)^2 - (v_2')^2 = (u_1)^2 - (u_2')^2 \quad (18)$$

or $(v_2')^2 = (u_2')^2 - (u_1)^2 = (v_1)^2$

but $v_2' = v_1(s_1/s_2) = v_1(r_1/r_2) \sin \beta_1$ (19)

and $u_2' = u_1(r_2/r_1)$

Calling $x = (r_2/r_1)^2$

$$x^2 - [1 - (v_1/u_1)^2]x - (v_1/u_1)^2 \sin^2 \beta_1 = 0 \quad (20)$$

If the ideal velocity of wheel $u_1 = \frac{1}{2}V_1 \cos \alpha_1$

then $v_1/u_1 = 1/\cos \beta_1$ (21)

Assuming $\alpha_1 = 16^\circ$, $\beta_1 = 30^\circ$

then $v_1/u_1 = 1/0.866 = 1.15$

$$(v_1/u_1)^2 = 1.33, \text{ approx.}$$

$$1 - (v_1/u_1)^2 = -0.33; \sin^2 \beta_1 = 1/4$$

Then equation (20) becomes

$$x^2 + 0.33x - 0.332 = 0$$

$$x = 0.435$$

$$x^{1/2} = r_2/r_1 = 0.66$$

$$2r_1 = D_1$$

Therefore $a = 0.17D_1 = \text{radial rim width.}$ (22)

$D_1 = \text{the outside diameter of the wheel.}$

This value of (a), the radial rim width, was graphically ascertained from the intersection of the two curves (Figure 5).

$$(v_2')^2 = (r_2/r_1)^2(u_1)^2 + (v_1)^2 - (u_1)^2 \quad (18)$$

and $v_2' = v_1(r_1/r_2) \sin \beta_1$ (19)

$$\boxed{v_2' = v_1(r_1/r_2) \sin \beta_1}$$

↗
CONTINUITY

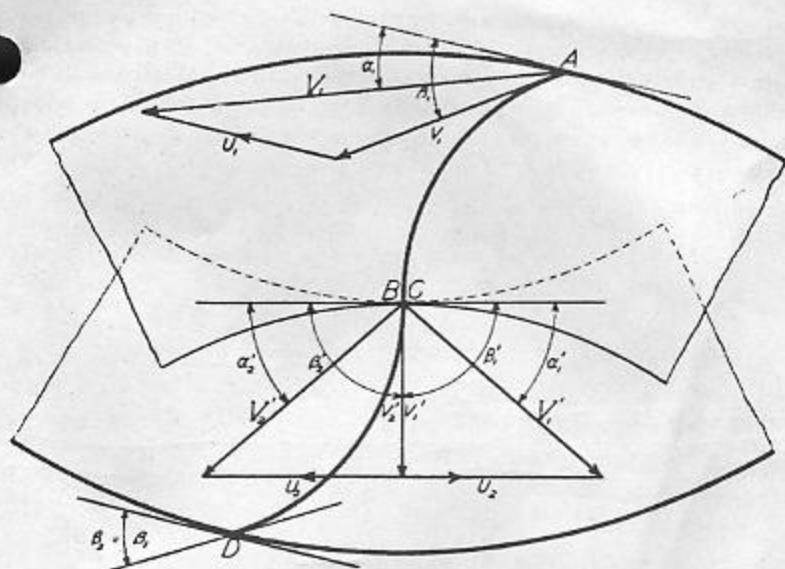


Figure 6. Composite velocity diagram.

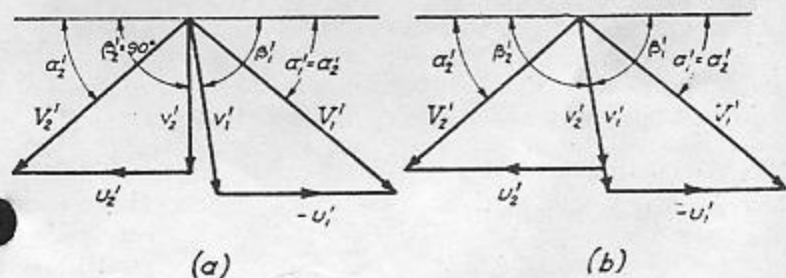


Figure 7. Velocity diagrams.

Assuming $\beta_2 = 90^\circ$ the inner exit blade spacing is known for every rim width. (a),

$$s_2 = t(r_2/r_1) \quad (16)$$

As long as (a) is small the space between the blades will not be filled by the jet. As (a) increases s_2 decreases so (a) will be limited by

$$s_2 = r_1 s_1 / r_2' \quad (17)$$

The central angle bOC , Figure 8, can be determined from equation (18) and

$$\alpha_2' = bOC/2$$

$$v_1 = u_1/\cos B_1 = u_1/0.866$$

$$r_2/r_1 = 0.66$$

$$v_2' = u_1[(0.66)^2 + 1.33 - 1]^{1/2}$$

$$= 0.875u_1$$

$$(23)$$

$$\tan \alpha_2' = v_2'/u_2'$$

$$(24)$$

$$= 0.875u_1/0.66u_1$$

$$= 1.326$$

$$\alpha_2' = 53^\circ$$

$$\text{angle } bOC = 106^\circ$$

$$(25)$$

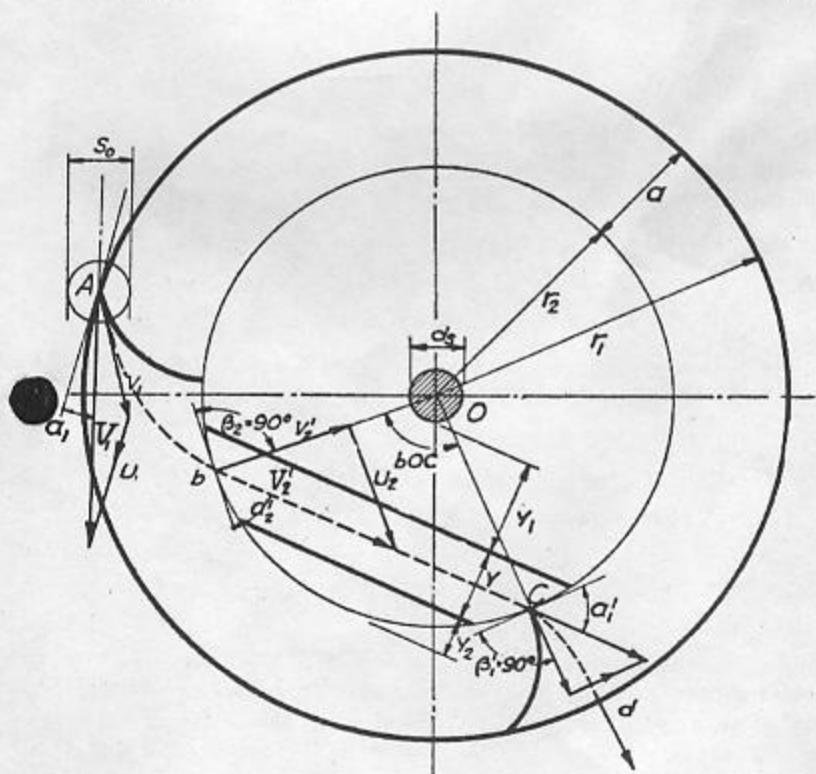


Figure 8. Path of jet inside wheel.

The thickness of the jet (y) in the inner part of the wheel can be computed from the continuity equation of flow (Figure 8),

$$V_1 s_0 = V_2' y \quad (26)$$

$$\begin{aligned} V_2' \cos \alpha_2' &= u_2' = (r_2/r_1) u_1 \\ &= (r_2/r_1) V_1/2 \cos \alpha_1 \end{aligned}$$

therefore, $y = 2 \cos \alpha_2' s_0 / (r_2/r_1) \cos \alpha_1$ (27)

$$\begin{aligned} &= (3.03)(0.6) s_0 / 0.961 \\ &= 1.89 s_0 \end{aligned} \quad (28)$$

The distance between the inside edge of the inside jet as it passes through the wheel and the shaft of the wheel, y_1 (Figure 8),

$$y_1 = r_2 \sin(90 - \alpha_2') - 1.89 s_0 / 2 - d/2 \quad (29)$$

since $s_1 = k D_1$
then $y_1 = (0.1986 - 0.945k) D_1 - d/2$ (30)

In a similar manner the distance y_2 , the distance between the outer edge of the jet and the inner periphery, can be determined.

$$y_2 = (0.1314 - 0.945k) D_1 \quad (31)$$

For the case where the shaft does not extend through the wheel, the only limit will be y_2 .

For most cases $k = 0.075$ to 0.10

then $y_1 + d/2 = 0.128 D_1$ to $0.104 D_1$
 $y_2 = 0.0606 D_1$ to $0.0369 D_1$

(C) Wheel diameter and axial wheel breadth: The wheel diameter can be determined from the following equation,

$$u_1 = \pi D_1 N / (12) \quad (60) \quad (32)$$

$$(1/2) V_1 \cos \alpha_1 = \pi D_1 N / (12) \quad (60)$$

$$\begin{aligned} (1/2) C (2gH)^{1/2} \cos \alpha_1 &= \pi D_1 N / (60) \quad (12) \\ D_1 &= 360 C (2gH)^{1/2} \cos \alpha_1 / \pi N \end{aligned} \quad (33)$$

Where D_1 is the diameter of the wheel in inches and $\alpha_1 = 16^\circ$, $C = 0.98$

$$D_1 = 862 H^{1/2} / N \quad (34)$$

The thickness s_0 of the jet in the nozzle is dependent upon a compromise of two conditions. A large value for s_0 would be advantageous because the loss caused by the filling and emptying of the wheel would be small. However, it would not be satisfactory because the

angle of attack of the outer filaments of the jet would vary considerably from $\alpha_1 = 16^\circ$, thereby increasing these losses as the thickness increased. The thickness should be determined by experiment.

In finding the breadth of the wheel (L), the following equations are true:

$$Q = (C_{s_0}L/144)(2gH)^{\frac{1}{2}} \quad (35)$$

$$= C(kD_1L/144)(2gH)^{\frac{1}{2}}$$

$$D_1 = 144Q/CkL(2gH)^{\frac{1}{2}} \\ = (862/N)H^{\frac{1}{2}} \quad (34)$$

$$144Q/CkL(2gH)^{\frac{1}{2}} = (862/N)H^{\frac{1}{2}}$$

$$L = 144QN/862H^{\frac{1}{2}}Ck(2gH)^{\frac{1}{2}} \\ = 0.283QN/H \text{ to } 0.212QN/H \quad (36)$$

where $k = 0.075$ and 0.10 respectively.

(D) Curvature of the blade: The curve of the blade can be chosen from a circle whose center lies at the intersection of two perpendiculars, one to the direction of relative velocity v_1 at (A) and the other to the tangent to the inner periphery intersecting at (B) (Figure 9).

From triangles AOC and BOC , \overline{CO} is common,

$$\text{then } (\overline{OB})^2 + (\overline{BC})^2 = (\overline{AO})^2 + (\overline{AC})^2 - 2\overline{AO}\overline{AC}\cos\beta_1$$

$$\text{but } \overline{AO} = r_1$$

$$\overline{OB} = r_2$$

$$\overline{AC} = \overline{BC} = \rho$$

$$\rho = [(r_1)^2 - (r_2)^2]/2r_1\cos\beta_1$$

$$\text{When } r_2 = (0.66r_1); \text{ and } \cos\beta_1 = \cos 30^\circ = 0.866,$$

$$\rho = 0.326r_1 \quad (37)$$

(E) Central angle:

$$r_1/r_2 = \sin(180^\circ - \frac{1}{2}\delta)/\sin(90^\circ - (\frac{1}{2}\delta + \beta_1)) \\ = \sin\frac{1}{2}\delta/\cos(\frac{1}{2}\delta + \beta_1)$$

$$\tan\frac{1}{2}\delta = \cos\beta_1/(\sin\beta_1 + r_2/r_1)$$

$$\delta = 73^\circ 28'$$

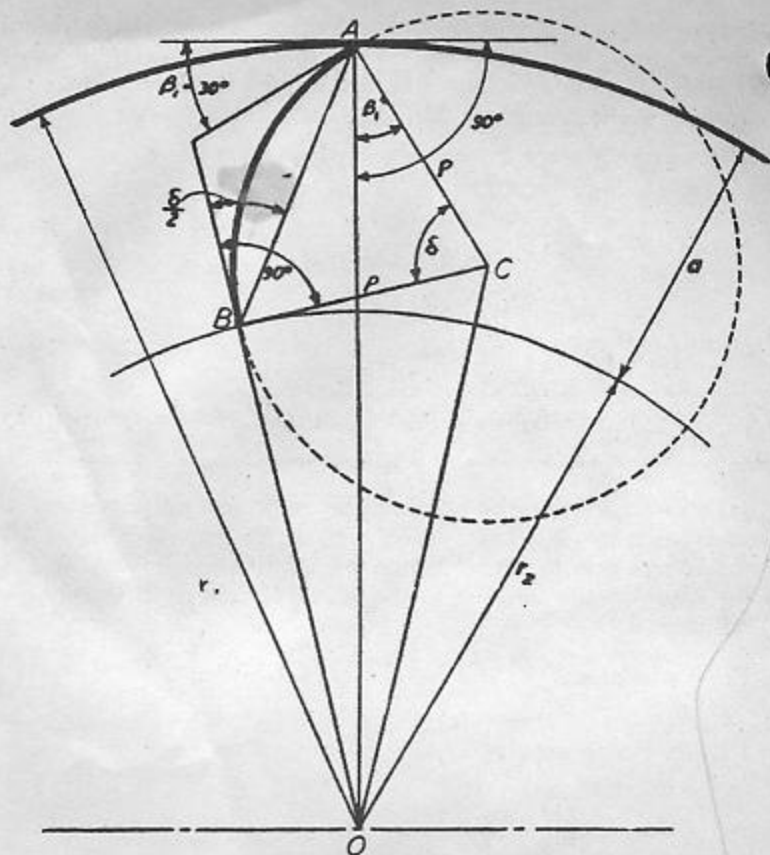


Figure 9. Curvature of blades.

III. DESIGN OF LABORATORY TURBINE

1. **Assumed design data.** From the foregoing discussion by Dr. Banki, a small turbine was designed, constructed, and tested at the Oregon State College hydraulics laboratory. The following assumptions were made subject to the conditions existing in the laboratory. All computations are made for the operation of the turbine at maximum efficiency.

Given $N_s = 14.0$
 $H = 16.0$ ft
 $Q = 3.0$ cfs

Assume $e = 55$ per cent for a small wheel

then $HP = QHe/8.8 = (3.0)(16)(0.55)/8.8 = 3.0$

2. **Breadth and diameter of wheel.** If $C=0.98$ and $k=0.087$, the latter being the mean of the values given by Dr. Banki,

$$L = 144 QN / (862)(0.98)(0.087)(2g)^{1/2} H = 0.244 QN/H \quad (36)$$

but $N = (862/D_1)H^{1/2} \quad (34)$

then $L = 144 Q / (0.98)(0.087)(2g)^{1/2} D_1 H^{1/2} = 210.6 Q / D_1 H^{1/2}$
 $LD_1 = (210.6)(3.0)/(16)^{1/2} = 158$

L (Inches)	D_1 (Inches)
10	15.8
11	14.4
12	13.1
13	12.1
14	11.3

Let $L = 12''$ be selected, then $D_1 = 13.1''$. If any other breadth be chosen, N , D_1 , s_0 , and t would be affected accordingly.

3. Speed of wheel.

$$N = (862/D_1)H^{1/2} \quad (34)$$

$$= (862/13.1)(16)^{1/2} = 263 \text{ rpm.}$$

4. **Thickness of jet.** Area of jet $= Q/V = 3.0 / (.98)(8.02)(4) = 0.094$ sq ft

$$s_0 = A/L = (0.094)(144)/12 = 1.13''$$

5. Spacing of blades in wheel.

$$s_1 = kD_1 = (0.087)(13.1) = 1.14''$$

$$t = s_1 / \sin \beta = 1.14 / 0.5 = 2.28'' \quad (15)$$

If only one blade at a time be assumed as cutting the jet, so that the blade spacing, t , be as shown in Figure 5, then the number of blades, n , is

$$n = \pi D_1 / t = \pi(13.1) / 2.28$$

$$= 18.1 \quad (20 \text{ were used for this experiment})$$

31416

$$\begin{array}{r} 6.5 \\ 2 \overline{) 13.1} \\ \underline{12} \\ 110 \\ \underline{104} \\ 60 \\ \underline{58} \\ 20 \end{array}$$

$$\begin{array}{r} 6.5 \\ 2 \overline{) 13.1} \\ \underline{12} \\ 110 \\ \underline{104} \\ 60 \\ \underline{58} \\ 20 \end{array}$$

This may not be the proper number of blades for maximum efficiency. Fewer blades may cause pulsating power, while a larger number of blades may cause excessive friction loss. The optimum number can be found only by experiment.

6. Radial rim width.

$$\begin{aligned} a &= 0.17 D_1 & (22) \\ &= (0.17)(13.1) \\ &= 2.22 \text{ inches} \end{aligned}$$

7. Radius of blade curvatures.

$$\begin{aligned} \rho &= 0.326 r_1 \quad \text{Figure 9} & (37) \\ &= 2.14 \text{ inches} \end{aligned}$$

8. Distance of jet from center of shaft.

$$\begin{aligned} y_1 &= (0.1986 - 0.945k) D_1 & (30) \\ &= 1.5 \text{ inches} \end{aligned}$$

9. Distance of jet from inner periphery of wheel.

$$\begin{aligned} y_2 &= (0.1314 - 0.945k) D_1 & (31) \\ &= 0.64 \text{ inches} \end{aligned}$$

10. Construction of the wheel. The wheel was constructed at the College by senior students under the direction of the authors. The side disks of the wheel were cut out of 1/4 inch steel plate. The blades were made of 7/64 inch steel, bent on an arc of a curve whose radius was 2.14 inches. The blades were placed between the disks in grooves spaced 2.08 inches apart around the outer periphery and brazed to the disks. The wheel was mounted on a one-inch steel shaft and keyed. The shaft was set in three ball bearing rings mounted in a housing of angle irons set on a heavy wooden framework. The nozzle was built up of sheet iron with a slide valve operating parallel to the rotor axis on a ratchet. This valve was manually controlled so that the width of the jet could be controlled at will, while the jet thickness and the angle α_1 remained constant.

11. Laboratory tests. Thorough tests were made on the wheel in the hydraulics laboratory at Oregon State College. The nozzle was attached to a large pressure tank and the head regulated on the nozzle by means of eight, four, and one inch gate valves. All the water was

furnished by two centrifugal pumps. The head on the nozzle was measured by direct piezometer readings. The brake load was obtained by a Prony brake, with a two-foot lever arm on tested weighing scales. The water used by the turbine was weighed in tanks connected to Toledo scales. The tests were made on about five different occasions by the authors and students, and in each case every measuring device was thoroughly calibrated before being used. The following heads, measured to the center of the rotor, were used: 9, 10, 12, 14, 16, and 18 feet. The velocity of approach in the nozzle for the gate openings of full, three-quarter, one-half, one-quarter, and one-eighth varied from a maximum to a minimum. In order to bring the results to a common basis for discussion the total head, pressure plus velocity head, was reduced to a common base of 9, 10, 12, 14, 16, and 18 feet. Data were taken at speed increments of 25 rpm from 0 to maximum.

IV. DISCUSSION

1. **Limitations of tests.** The curves shown in this paper, figures 10, 11, and 12, are limited to the test on the turbine under a sixteen foot head for various gate openings. The results of the tests at the heads mentioned previously are discussed.

2. **Power.** The maximum power developed was 2.75 at 280 rpm at full gate, Figure 10. The power is slightly lower than the anticipated power, while the speed is slightly in excess of the optimum speed. The amount of water used is only 2.22 cfs in place of 3.0 cfs as assumed. The maximum power obtained with the smaller gate openings was practically in proportion to the gate openings. Power developed under the other heads at the optimum speeds is in direct proportion to the three halves power of the heads involved.

Head in ft	9	10	12	14	16	18
Actual bhp	1.17	1.40	1.80	2.25	2.75	3.30
Computed by head ratio	1.19	1.39	1.82	2.30		3.31

3. **Quantity.** The quantity of water used under a 16 foot head was only 2.22 cfs in place of the assumed 3.0 cfs. A slight decrease in the size of the jet thickness would cause a corresponding decrease in the quantity. The jet thickness actually measured after the nozzle was built was 1.05 inches. Lack of jigs and proper equipment made the work of building the nozzle to very accurate dimensions rather

difficult, and probably increased nozzle losses with a resultant lower nozzle coefficient than that assumed.

A slight decrease in quantity occurred with an increase in speed.

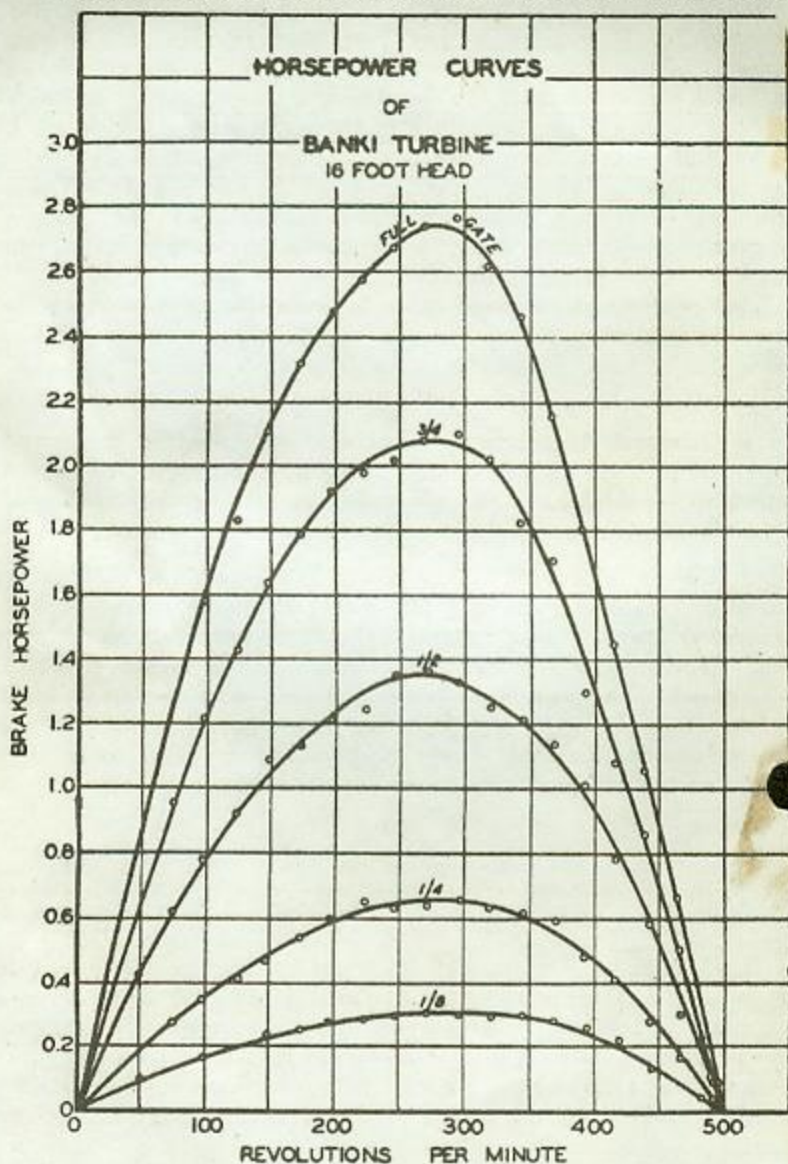


Figure 10. Power curves for Banki turbine under 16-ft head.

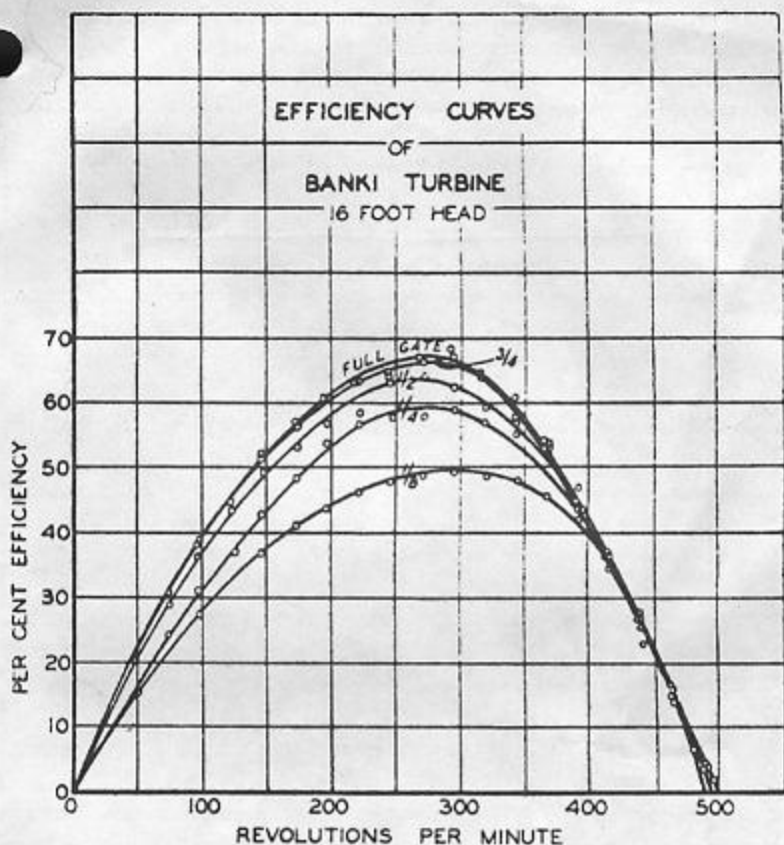


Figure 11. Efficiency curves for Banki turbine under 16-ft head.

4. **Speed.** According to the power-speed, Figure 10, and efficiency-speed, Figure 11, curves, the speed for maximum power for all gate openings from one-eighth to full under 16-foot head was practically constant. The computed speed was 263 rpm and the actual speed determined by experiment was 270 rpm. The optimum speed for maximum power at the other heads is shown below.

Head in ft	9	10	12	14	16	18
Actual rpm	197	212	232	260	270	290
Computed	202	212	234	253		287

5. **Efficiency-speed.** The highest efficiency attained was 68 per cent at optimum speed of 270 rpm, Figure 11. The efficiency decreased with the decrease in gate opening. Maximum efficiency for one-eighth gate opening was 50 per cent. The efficiency of the

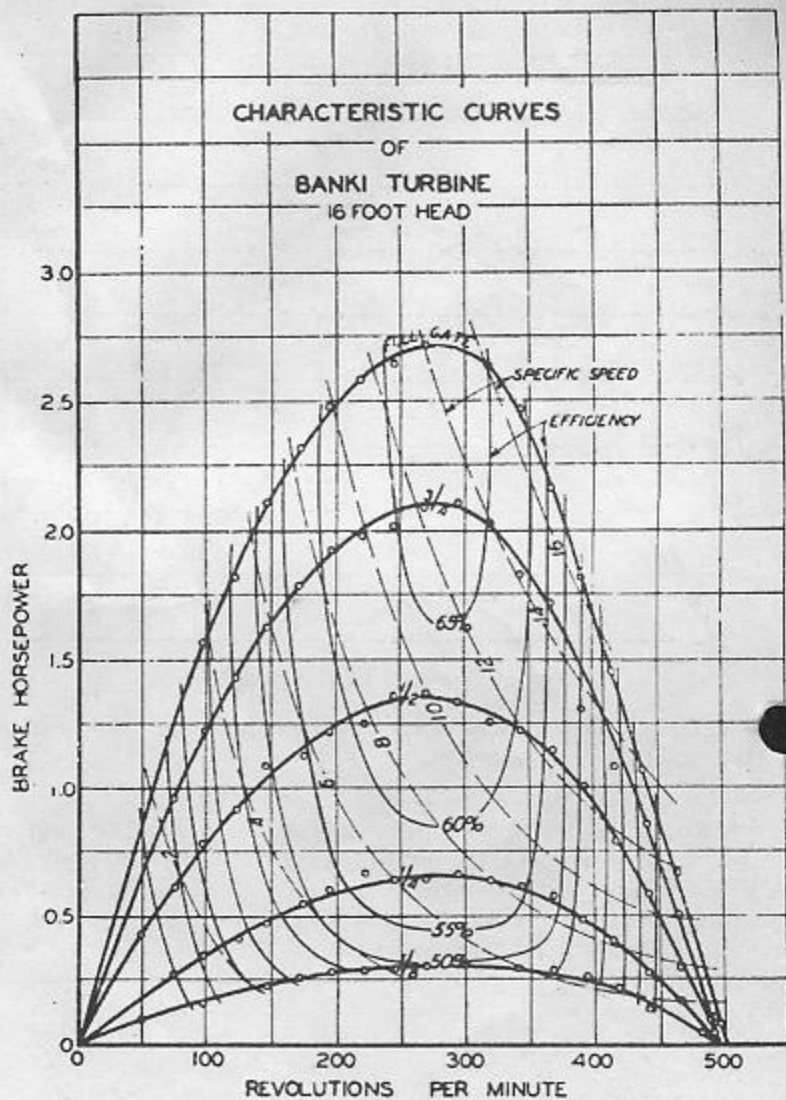


Figure 12. Characteristic curves for Banki turbine under 16-ft head.

turbine was maintained over a wide range of speeds. The maximum efficiency was practically constant at full gate openings for all the heads.

6. **Efficiency-power.** A curve of efficiency-power would present a fairly high range of efficiencies over a large range in power. This range is relatively wider than those generally obtained from tangential, reaction, or propeller turbines.

7. **Specific speed.** The characteristic curves of the turbines at 16 foot head, Figure 11, show that the specific speed varies from 2 to 16. The specific speed at maximum efficiency is 14. The turbine could be operated efficiently over a range of 6 to 16 specific speed, a range which fills the gap between the tangential and mixed-flow turbines.

V. THE TURBINE NOZZLE

1. **Test nozzle.** A laboratory test nozzle was built and installed as shown in Figure 13. This nozzle was so arranged that the width of the jet remained constant. This had the same effect as reducing the effective length of the turbine runner as the demand for power became less. This necessitated the use of a pinion gear to actuate the mechanism to reduce or increase the width of the jet, and this of necessity reduced the speed with which such action could take place.

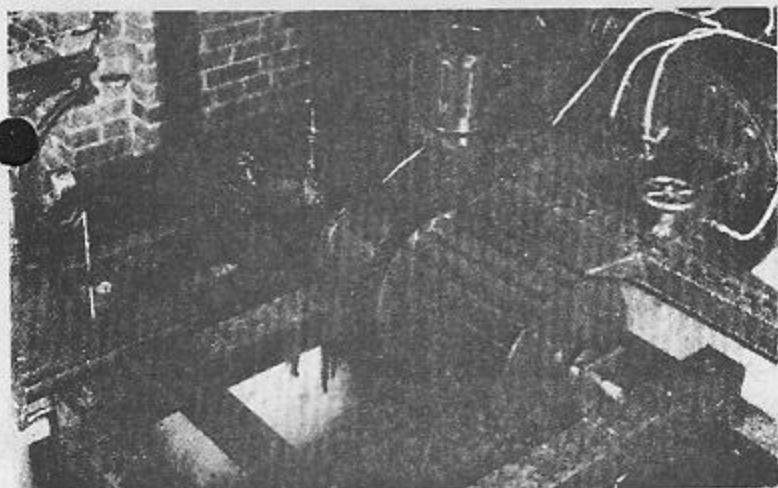


Figure 13. Banki water turbine built in Oregon State College Hydraulics Laboratory.

2. **German nozzles.** Instead of increasing or reducing the width of the jet for change in power requirements, the thickness of the jet could be changed. This method has been used with German patents, as shown in Figures 14 and 15. In Figure 14, a lever is attached to the gate A and actuated by the turbine governor. At C the water is forced to enter the turbine blades at the required angle for best operating efficiency, regardless of the flow of water. In Figure 15, the thickness of the jet may be changed by a slightly different patented device. The effect is the same as before.

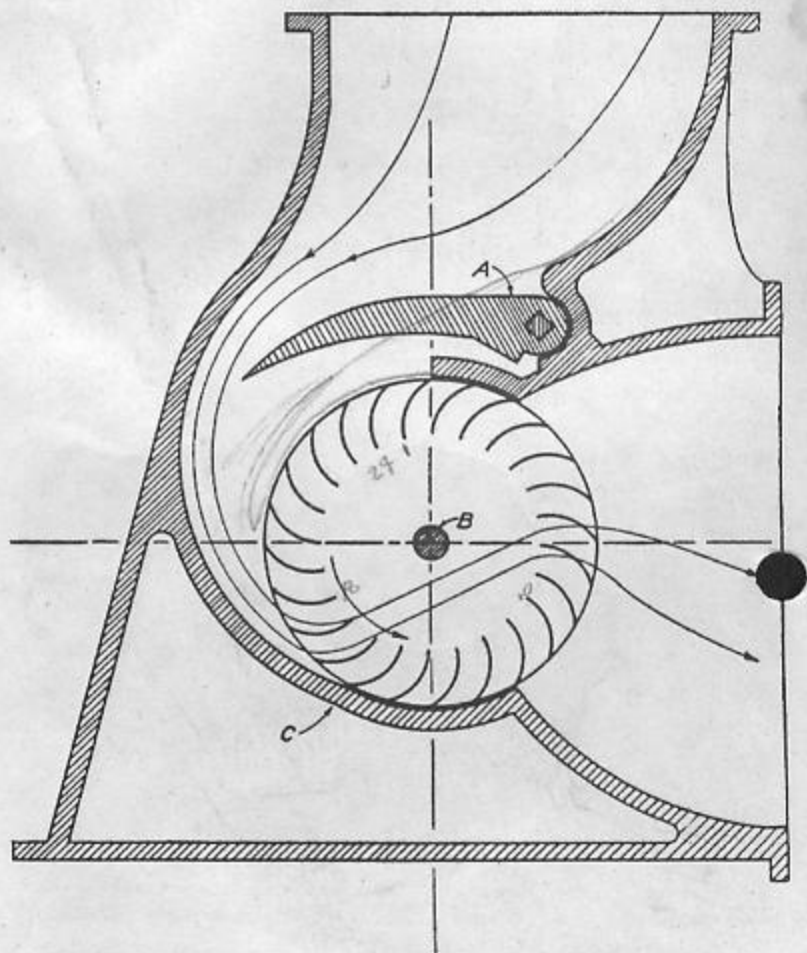


Figure 14. German design of Banki turbine and nozzle.

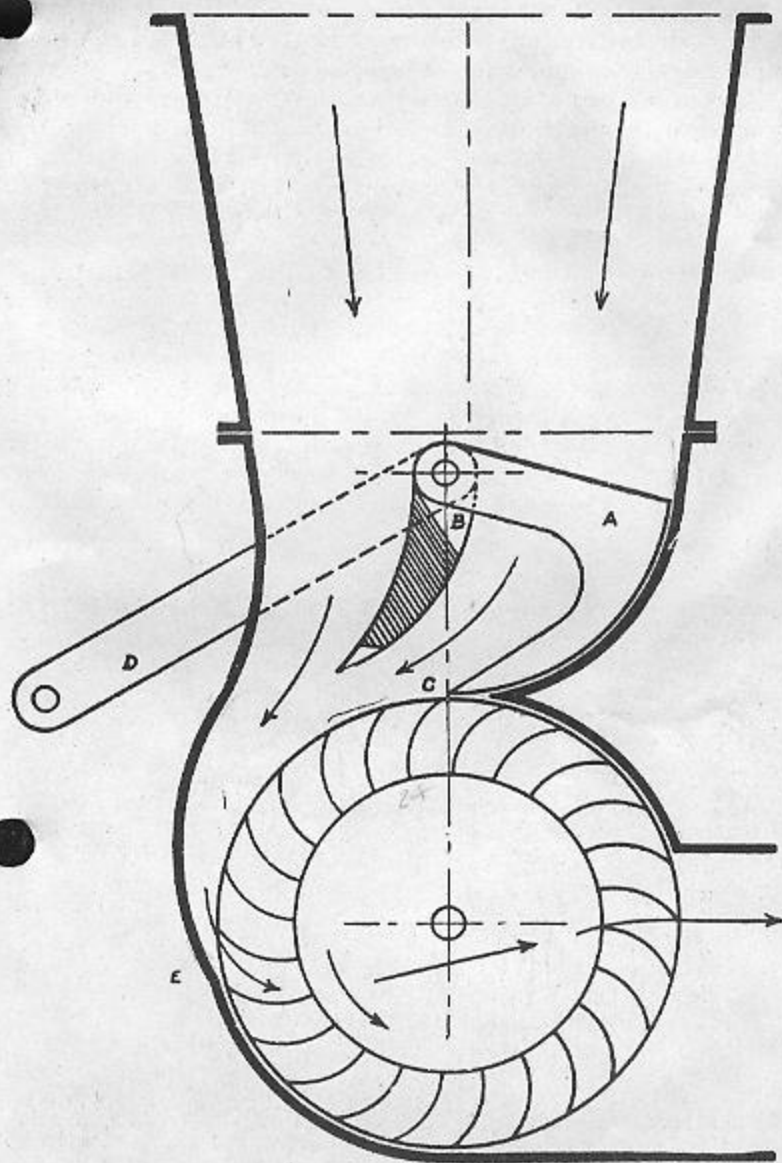


Figure 15. Alternate German design of Banki turbine and nozzle.

VI. INSTALLATIONS

1. **European turbines.** There seems to be a large number of Banki turbines installed in Europe. Commercial catalogs were available from Ganz & Co. before World War II, a firm which had installed many turbines throughout Europe.

2. **American installations.** Many Banki turbines have been installed in Oregon since the laboratory tests described in this bulletin were made. At least two different manufacturers have been building these water turbines, and many have been made in local shops.

The installation is simple, as shown in Figures 16, 17, and in Figure 1. A small wooden dam may be built across a small stream, the water diverted into a wooden flume where a head of 10 to 20 feet may be obtained. Near the end of the flume a vertical box, or penstock, may be constructed so that the turbine nozzle may be bolted to it. When the turbine is not in use, the water simply discharges over the end of the flume as shown. A small shed houses the electric generator and any necessary belting or other miscellaneous equipment.

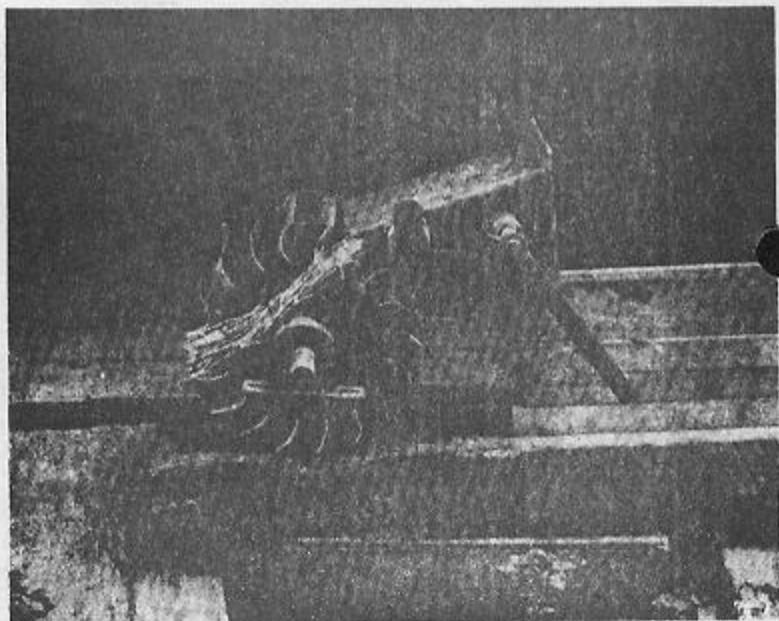


Figure 16. Banki turbine runner and nozzle.

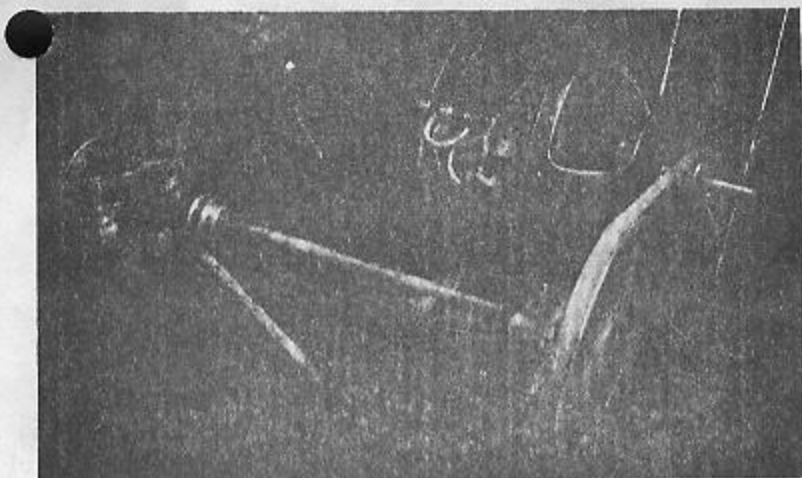


Figure 17. Inside of powerhouse, showing jackshaft and generator driven by Banki turbine.

VII. CONCLUSIONS

The test on the laboratory Banki turbine indicates that:

1. This turbine can be operated efficiently on a wider range of openings than most turbines.
2. Brake-horsepower varies almost directly with the three-halves power of the head.
3. Maximum efficiency occurs at practically a constant speed for all gate openings at constant head.

The Banki turbine characteristic speed occupies a position between those for the tangential and reaction turbines.

5. The effective width of the wheel can be changed at will without changing the angle of attack, (α).

It is felt that considerably more efficiency could be obtained by experimenting with different numbers of blades and different nozzles. An efficiency of 68 per cent is not extraordinary and one should not expect to have attained the maximum efficiency with one test, especially on a turbine of such small horsepower. Losses of water to the turbine were known; it is estimated that some 8 per cent of the total water never touched the wheel. Slight changes in design would reduce this loss considerably and thereby increase its efficiency.

It is obvious that there is a distinct place for the Banki turbine in the small turbine field. The advantages are simplicity and economy of construction.

**OREGON STATE COLLEGE
ENGINEERING EXPERIMENT STATION
CORVALLIS, OREGON**

LIST OF PUBLICATIONS

Bulletins—

- No. 1. Preliminary Report on the Control of Stream Pollution in Oregon, by C. V. Langton and H. S. Rogers. 1929.
Fifteen cents.
- No. 2. A Sanitary Survey of the Willamette Valley, by H. S. Rogers, C. A. Mockmore, and C. D. Adams. 1930.
Forty cents.
- No. 3. The Properties of Cement-Sawdust Mortars, Plain, and with Various Admixtures, by S. H. Graf and R. H. Johnson. 1930.
Twenty cents.
- No. 4. Interpretation of Exhaust Gas Analyses, by S. H. Graf, G. W. Gleeson, and W. H. Paul. 1934.
Twenty-five cents.
- No. 5. Boiler-Water Troubles and Treatments with Special Reference to Problems in Western Oregon, by R. E. Summers. 1935.
None available.
- No. 6. A Sanitary Survey of the Willamette River from Sellwood Bridge to the Columbia, by G. W. Gleeson. 1936.
Twenty-five cents.
- No. 7. Industrial and Domestic Wastes of the Willamette Valley, by G. W. Gleeson and F. Merryfield. 1936.
Fifty cents.
- No. 8. An Investigation of Some Oregon Sands with a Statistical Study of the Predictive Values of Tests, by C. E. Thomas and S. H. Graf. 1937.
Fifty cents.
- No. 9. Preservative Treatments of Fence Posts.
1938 Progress Report on the Post Farm, by T. J. Starker. 1938.
Twenty-five cents.
Yearly progress reports, 9-A, 9-B, 9-C, 9-D, 9-E, 9-F, 9-G.
Fifteen cents each.
- No. 10. Precipitation-Static Radio Interference Phenomena Originating on Aircraft, by E. C. Starr, 1939.
Seventy-five cents.
- No. 11. Electric Fence Controllers with Special Reference to Equipment Developed for Measuring Their Characteristics, by F. A. Everest. 1939.
Forty cents.
- No. 12. Mathematics of Alignment Chart Construction without the Use of Determinants, by J. R. Griffith. 1940.
Twenty-five cents.
- No. 13. Oil Tar Creosote for Wood Preservation, by Glenn Voorhies, 1940.
Twenty-five cents.
- No. 14. Optimum Power and Economy Air-Fuel Ratios for Liquefied Petroleum Gases, by W. H. Paul and M. N. Popovich. 1941.
Twenty-five cents.
- No. 15. Rating and Care of Domestic Sawdust Burners, by E. C. Willey. 1941.
Twenty-five cents.
- No. 16. The Improvement of Reversible Dry Kiln Fans, by A. D. Hughes. 1941.
Twenty-five cents.
- No. 17. An Inventory of Sawmill Waste in Oregon, by Glenn Voorhies. 1942.
Twenty-five cents.
- No. 18. The Use of Fourier Series in the Solution of Beam Problems, by B. F. Ruffner. 1944.
Fifty cents.
- No. 19. 1945 Progress Report on Pollution of Oregon Streams, by Fred Merryfield and W. G. Wilmot. 1945.
Forty cents.
- No. 20. The Fishes of the Willamette River System in Relation to Pollution, by R. E. Dimick and Fred Merryfield. 1945.
Forty cents.
- No. 21. The Use of the Fourier Series on the Solution of Beam-Column Problems, by B. F. Ruffner. 1945.
Twenty-five cents.

- No. 22. Industrial and City Wastes, by Fred Merryfield, W. B. Bollen, and F. C. Kachelhoffer. 1947.
Forty cents.
- No. 23. Ten-Year Mortar Strength Tests of Some Oregon Sands, by C. E. Thomas and S. H. Graf. 1948.
Twenty-five cents.
- No. 24. Space Heating by Electric Radiant Panels and by Reverse Cycle, by Louis Slegel. July 1948.
Fifty cents.
- No. 25. The Banki Water Turbine, by C. A. Mockmore and Fred Merryfield. February 1949.
Forty cents.

Circulars—

- No. 1. A Discussion of the Properties and Economics of Fuels Used in Oregon, by C. E. Thomas and G. D. Keerins. 1929.
Twenty-five cents.
- No. 2. Adjustment of Automotive Carburetors for Economy, by S. H. Graf and G. W. Gleeson. 1930.
None available.
- No. 3. Elements of Refrigeration for Small Commercial Plants, by W. H. Martin. 1935.
None available.
- No. 4. Some Engineering Aspects of Locker and Home Cold-Storage Plants, by W. H. Martin. 1938.
Twenty cents.
- No. 5. Refrigeration Applications to Certain Oregon Industries, by W. H. Martin. 1940.
Twenty-five cents.
- No. 6. The Use of a Technical Library, by W. E. Jorgensen. 1942.
Twenty-five cents.
- No. 7. Saving Fuel in Oregon Homes, by E. C. Willey. 1942.
Twenty-five cents.
- No. 8. Technical Approach to the Utilization of Wartime Motor Fuels, by W. H. Paul. 1944.
Twenty-five cents.
- No. 9. Electric and Other Types of House Heating Systems, by Louis Slegel. 1946.
Twenty-five cents.
- No. 10. Economics of Personal Airplane Operation, by W. J. Skinner. 1947.
Twenty-five cents.
- No. 11. Digest of Oregon Land Surveying Laws, by C. A. Mockmore, M. P. Coopey, B. B. Irving, and E. A. Buckhorn. 1948.
Twenty-five cents.

Reprints—

- No. 1. Methods of Live Line Insulator Testing and Results of Tests with Different Instruments, by F. O. McMillan. Reprinted from 1927 Proc. N. W. Elec. Lt. and Power Assoc.
Twenty cents.
- No. 2. Some Anomalies of Siliceous Matter in Boiler Water Chemistry, by R. E. Summers. Reprinted from Jan. 1935, Combustion.
Ten cents.
- No. 3. Asphalt Emulsion Treatment Prevents Radio Interference, by F. O. McMillan. Reprinted from Jan. 1935, Electrical West.
None available.
- No. 4. Some Characteristics of A-C Conductor Corona, by F. O. McMillan. Reprinted from Mar. 1935, Electrical Engineering.
None available.
- No. 5. A Radio Interference Measuring Instrument, by F. O. McMillan and H. G. Barnett. Reprinted from Aug. 1935, Electrical Engineering.
Ten cents.
- No. 6. Water-Gas Reaction Apparently Controls Engine Exhaust Gas Composition, by G. W. Gleeson and W. H. Paul. Reprinted from Feb. 1936, National Petroleum News.
Ten cents.
- No. 7. Steam Generation by Burning Wood, by R. E. Summers. Reprinted from April 1936, Heating and Ventilating.
Ten cents.
- No. 8. The Piezo Electric Engine Indicator, by W. H. Paul and K. R. Eldredge. Reprinted from Nov. 1935, Oregon State Technical Record.
Ten cents.

- No. 9. Humidity and Low Temperature, by W. H. Martin and E. C. Willey. Reprinted from Feb. 1937, *Power Plant Engineering*.
None available.
- No. 10. Heat Transfer Efficiency of Range Units, by W. J. Walsh. Reprinted from Aug. 1937, *Electrical Engineering*.
None available.
- No. 11. Design of Concrete Mixtures, by I. F. Waterman. Reprinted from Nov. 1937, *Concrete*.
None available.
- No. 12. Water-wise Refrigeration, by W. H. Martin and R. E. Summers. Reprinted from July 1938, *Power*.
None available.
- No. 13. Polarity Limits of the Sphere Gaps, by F. O. McMillan. Reprinted from Vol. 58, A.I.E.E. Transactions, Mar. 1939.
Ten cents.
- No. 14. Influence of Utensils on Heat Transfer, by W. G. Short. Reprinted from Nov. 1938, *Electrical Engineering*.
Ten cents.
- No. 15. Corrosion and Self-Protection of Metals, by R. E. Summers. Reprinted from Sept. and Oct. 1938, *Industrial Power*.
Ten cents.
- No. 16. Monocoque Fuselage Circular Ring Analysis, by B. F. Ruffner. Reprinted from Jan. 1939, *Journal of the Aeronautical Sciences*.
Ten cents.
- No. 17. The Photoelastic Method as an Aid in Stress Analysis and Structural Design, by B. F. Ruffner. Reprinted from Apr. 1939, *Aero Digest*.
Ten cents.
- No. 18. Fuel Value of Old-Growth vs. Second-Growth Douglas Fir, by Lee Gable. Reprinted from June 1939, *The Timberman*.
Ten cents.
- No. 19. Stoichiometric Calculations of Exhaust Gas, by G. W. Gleeson and F. W. Woodfield, Jr. Reprinted from November 1, 1939, *National Petroleum News*.
Ten cents.
- No. 20. The Application of Feedback to Wide-Band Output Amplifiers, by F. A. Everest and H. R. Johnston. Reprinted from February 1940, *Proc. of the Institute of Radio Engineers*.
Ten cents.
- No. 21. Stresses Due to Secondary Bending, by B. F. Ruffner. Reprinted from Proc. of First Northwest Photoelasticity Conference, University of Washington, March 30, 1940.
Ten cents.
- No. 22. Wall Heat Loss Back of Radiators, by E. C. Willey. Reprinted from November 1940, *Heating and Ventilating*.
- No. 23. Stress Concentration Factors in Main Members Due to Welded Stiffeners, by W. R. Cherry. Reprinted from December, 1941, *The Welding Journal, Research Supplement*.
Ten cents.
- No. 24. Horizontal-Polar-Pattern Tracer for Directional Broadcast Antennas, by F. A. Everest and W. S. Pritchett. Reprinted from May, 1942, *Proc. of the Institute of Radio Engineers*.
Ten cents.
- No. 25. Modern Methods of Mine Sampling, by R. K. Meade. Reprinted from January, 1942, *The Compass of Sigma Gamma Epsilon*.
Ten cents.
- No. 26. Broadcast Antennas and Arrays. Calculation of Radiation Patterns; Impedance Relationships, by Wilson Pritchett. Reprinted from August and September, 1944, *Communications*.
Fifteen cents.
- No. 27. Heat Losses Through Wetted Walls, by E. C. Willey. Reprinted from June, 1946, *ASHVE Journal Section of Heating, Pipng, & Air Conditioning*.
Ten cents.
- No. 28. Electric Power in China, by F. O. McMillan. Reprinted from January, 1947, *Electrical Engineering*.
Ten cents.
- No. 29. The Transient Energy Method of Calculating Stability, by P. C. Magnusson. Reprinted from Vol. 66, A.I.E.E. Transactions, 1947.
Ten cents.
- No. 30. Observations on Arc Discharges at Low Pressures, by M. J. Kofoid. Reprinted from April, 1948, *Journal of Applied Physics*.
Ten cents.
- No. 31. Load-Range Planning for Power Supply, by F. O. McMillan. Reprinted from December, 1948, *Electrical Engineering*.
Ten cents.